processes

MDPI

Article

Performance Evaluation on Open-Graded Friction Course Reinforced by Double-Adding Fibers Technology

Cihe Chen [1,2], Chimou Li [1,3], Saibang Zhang [4], Wenchang Liu [5,6], Hongwei Lin [5,*] and Hongchao Zhang [5]

1 Wenshan Expressway Construction and Development of CCCC Co., Ltd., Wenshan 663099, China; cihechen@163.com (C.C.); chimouli@163.com (C.L.)
2 CCCC Western Investment Co., Ltd., Chengdu 610000, China
3 CCCC Second Harbor Engineering Company Ltd., Wuhan 430040, China
4 Yunnan Wenshan Transportation Investment Group Engineering Quality Testing Co., Ltd., Wenshan 663099, China; saibangzhang@163.com
5 Key Laboratory of Road and Traffic Engineering of Ministry of Education, Tongji University, Shanghai 201804, China; jackliu0306@163.com (W.L.); zhanghc@tongji.edu.cn (H.Z.)
6 Shanghai Fengxian Construction Development Group Co., Ltd., Shanghai 201401, China
* Correspondence: 2010750@tongji.edu.cn

Abstract: The use of an open-graded friction course (OGFC) as a road surface demonstrates significant advantages in reducing driving noise and improving road drainage and safety. This study aims to enhance the overall performance of OGFC-13 by incorporating double-adding fiber technology. Laboratory tests were conducted on six OGFC-13 mixes modified with varying fiber ratios of lignin fibers (LFs) and glass fibers (GFs). Both GF and LF significantly improved high-temperature performance, with dynamic stability values increasing proportionally to GF content. The LF:GF = 0.15:0.15 ratio achieved peak shearing strength, demonstrating better improvement over single-fiber modification. Furthermore, both fibers effectively enhanced resistance to cracking, with GF-reinforced specimens excelling in bending stress and LF-reinforced specimens demonstrating the highest flexural strain. Water stability evaluations highlighted the substantial positive impact of LF and GF, with simultaneous addition resulting in superior moisture stability compared to single-fiber modifications. Anti-stripping performance assessments indicated that the LF:GF = 3:0 ratio exhibited the best performance. In fatigue performance, both LF and GF enhanced fatigue life, with GF outperforming LF. The LF:GF = 0.15:0.15 ratio achieved a balanced fatigue performance. Results from the radar evaluation method underscored a more comprehensive improvement in road performance achieved through double-adding technology. The LF:GF = 0.15:0.15 ratio emerged as the optimal choice for overall road performance.

Keywords: asphalt mixture; OGFC; fiber modification; lignin fiber; glass fiber

Citation: Chen, C.; Li, C.; Zhang, S.; Liu, W.; Lin, H.; Zhang, H. Performance Evaluation on Open-Graded Friction Course Reinforced by Double-Adding Fibers Technology. *Processes* **2024**, *12*, 428. https://doi.org/10.3390/pr12030428

Received: 30 January 2024
Revised: 18 February 2024
Accepted: 19 February 2024
Published: 20 February 2024

1. Introduction

The maintenance of asphalt pavement is a challenge for transportation development in various countries around the world. Currently, China has around 5.35 million km of road under maintenance. Developed countries like the United States, Japan, and Europe also have numerous highways requiring maintenance on a global scale. Open-graded friction course (OGFC) is a popular preventative maintenance solution globally known for its exceptional cost-effectiveness. However, OGFC is susceptible to faults, including aggregate peeling, aging, and cracking over time, leading to a service life significantly less than its intended design life [1,2]. The characteristics of coarse grading and large voids in OGFC mixtures not only provide excellent road drainage and noise reduction functions but also have negative effects on its mechanical strength, aging resistance, water stability and other properties. Improving the road performance of OGFC is of great significance for extending road maintenance time and reducing road life cycle costs. Thus, certain technical

measures are required to strengthen and improve its performance. Fiber-reinforced OGFC mixtures are a viable technology.

Fiber is a frequently utilized material in modern asphalt pavements. It creates a solid three-dimensional reinforcement network by absorbing stable asphalt, offering bridging reinforcement, and integrating with the asphalt mixture. This process significantly improves the overall road performance of OGFC mixes [3,4]. The fibers can boost the amount of structural asphalt in asphalt mixtures, improve bonding strength, and reduce slide between aggregates. The addition methods of fibers into asphalt mixtures include wet and dry methods [5,6]. The wet method involves adding fibers to asphalt to prepare fiber-modified asphalt. Kou et al. studied the rheological behavior of a reinforced asphalt binder with different fiber types. They recommended the optimal content of shortcut basalt fiber, polyester fiber, lignin fiber (LF) and flocculent basalt fiber as 2%, 3%, 4% and 4%, respectively [7]. Similarly, Xing et al. investigated the impact of several fiber types on asphalt and determined that flocculent fibers stabilize asphalt, whereas bundle fibers improve toughness [8]. The essence of fiber-modified asphalt is to promote the colloidal structure of asphalt to change from a sol to a solution gel structure and perhaps to a gel structure. However, the wet approach is not widely utilized in engineering because of the limited compatibility between fibers and asphalt and the intricate preparatory process it entails. The dry approach entails incorporating a specific quantity of fibers into the asphalt mixture during mixing, followed by blending aggregates, fibers, and asphalt at high temperatures to create a fiber-modified asphalt mixture. A study by Partl et al. discovered that lignin fibers can enhance the mechanical characteristics of SMA. However, they also observed a fiber aggregation issue during the mixing procedure [9]. The distribution of fibers was improved through increasing the temperature and duration of mixing. Mahrez et al. recommended using a glass fiber (GF)-reinforced asphalt mixture after comparing various fiber applications, which lead to higher construction expenses but could also result in decreased maintenance costs [10]. The dry method is more favorable for achieving a uniform distribution of fibers in asphalt mixtures compared to the wet method, and it also involves a simpler preparation process [11,12]. Hence, the dry method is typically the preferred option for the majority of road engineering projects.

At present, different types of fibers are used in asphalt applications, categorized as plant fibers, synthetic fibers, and mineral fibers [3,13,14]. Variances in composition and volume characteristics lead to notable distinctions in the physical and chemical properties of fibers, thereby affecting their bonding affinity with asphalt. Various types of fibers offer unique benefits in enhancing the high-temperature, low-temperature, and fatigue properties of asphalt mixes. A study revealed that the effects of lignin, basalt, polyester, and polyacrylonitrile fibers in permeable mixtures can enhance their performance, indicating that fiber modification can improve the overall performance of the mixture [3,15]. However, different fiber types have different focuses in relation to improving performance, with polyester fibers being assessed as the best. Considering the differences in usage effects and economic benefits among different fiber types, researchers have begun to study double-adding fiber technology and achieved good results [16,17]. Sun investigated the reinforcement effect of basalt, lignin and polyester fibers in asphalt mortar [18]. The results indicated that the addition of polyester and basalt fiber exhibited better shear strength than that of basalt and lignin fiber. Abtahi found that using a 6% polypropylene fiber and 0.1% GF-modified asphalt mixture can effectively improve the stability of the mixture and reduce its fluidity [19]. Similarly, Khater et al. evaluated the effect of composite admixtures of LF and GF on the moisture damage and low-temperature cracking of AC-16 and found that the composite admixture outperformed both LF and GF individually [17]. However, existing research in the literature shows that there is currently no report on the application of double-adding fiber technology in OGFC mixes. Due to the open gradation and high porosity of OGFC mixes, it is worth exploring how to simultaneously apply different fibers with individual advantages and disadvantages to improve the overall road performances of OGFC-13 by leveraging the advantages of different fibers.

In view of this, this study aims at improving the overall road performances of OGFC using double-adding fiber technology. Glass fiber (GF) is a synthetic inorganic fiber with advantages such as high tensile strength and good mechanical properties. Therefore, the GF-reinforced asphalt mixture can improve asphalt's stability, durability and ductility [20,21]. The widespread production and commercial availability of GF in various industries, including construction and engineering, generally leads to competitive and reasonable pricing. Lignin fiber (LF) is a natural inorganic fiber with advantages inherent in its flocculation structure, rough surface and large specific surface area. It can significantly adsorb and stabilize asphalt, endowing asphalt mixtures with higher cohesion, viscosity, flexural and tensile strength and fatigue life [22–24]. LFs are derived from plant material, primarily wood. Currently, LF is readily accessible worldwide. The extraction and use of LF are in line with sustainable principles. GF and LF fibers are commonly utilized in civil engineering because they are readily accessible and cost-effective. Thus, two fibers, GF and LF, were chosen to find the ideal fiber ratio for OGFC mixtures. This study used a dry method to prepare a fiber-modified OGFC mixture by simultaneously adding LF and GF into the OGFC mixes. Extensive laboratory experiments were carried out to assess the effect of the double-adding technology of lignin and glass fiber on the road performances of OGFC-13 mixes. The research findings are relevant for enhancing the service performance of OGFC and offer a practical solution for optimizing preventative maintenance technology.

2. Experimental Design

2.1. Materials

2.1.1. Asphalt

A high-viscosity modified asphalt used in this research was provided by China Aviation Lutong Industrial Co., Ltd. (Guangzhou City, China). As shown in Table 1, the properties of the high-viscosity modified asphalt satisfy the technical requirements of Chinese Technical Specifications for Construction of Highway Asphalt Pavements (JTG F40-2004) [25].

Table 1. Properties of high viscosity modified asphalt.

Index	Penetration (25 °C)	Ductility (5 °C) (cm)	Softening Point (°C)
Test value	58	36	82.7
Standards	≥40	≥30	≥80

2.1.2. Aggregates

The mineral powder—the fine and coarse aggregates adopted in this study—is made of limestone, which was provided by Wenshan Prefecture, Yunnan Province. The technical indexes meet road technical requirements in the JTG F40-2004 Standard [25].

2.1.3. Fibers

Figure 1 displays the LF and GF used in this study provided by Jiangsu Zhongshi Fiber Co., Ltd. (Yancheng City, China). The physical properties of both fibers are presented in Table 2.

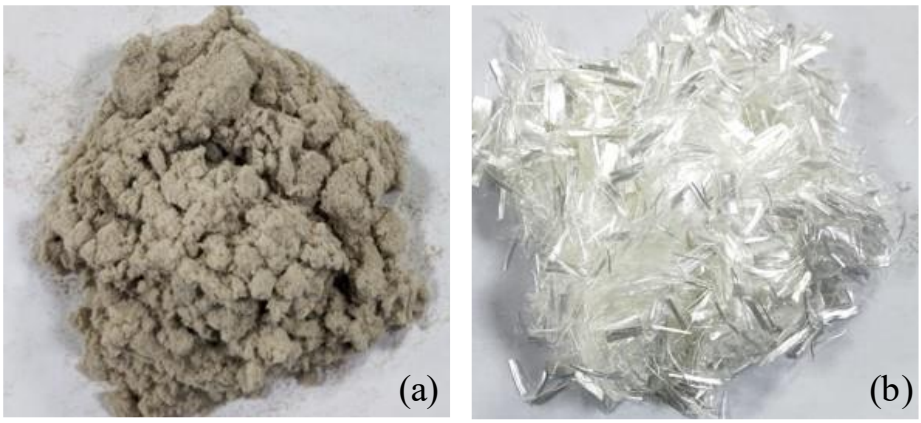

Figure 1. Fibers: (**a**) lignin fiber and (**b**) glass fiber.

Table 2. Properties of lignin fiber and glass fiber.

Property	Lignin Fiber	Glass Fiber
Appearance	Grey	White
Length (mm)	0.95	10
Diameter (mm)	0.05	0.010
Melting point (°C)	230	720
Tensile strength (MPa)	<300	2000
Elastic modulus (GPa)	3.0	70

2.2. Mixes Design

2.2.1. Fiber Content

The key to fiber modification technology lies in the determination of the fiber content. A study of a GF-reinforced asphalt mixture by Khater et al. proposed that the optimal proportion of GF for mixes was 0.3% of the total mass of the mix [17]. Similarly, the addition of 0.3% LF to the asphalt mixture was beneficial for water stability and low-temperature crack resistance [23]. Moreover, the JTG F40-2004 standard recommends that the LF content mixed into asphalt mixture is not less than 0.3% [25]. Based on this, the fiber content and ratio determined in this study are listed in Table 3.

Table 3. Fiber content and composite mixing ratio.

Group ID	Fiber Content	LF Content	GF Content
Control	0	0	0
0.3:0	0.3%	0.3%	0
0.2:0.1		0.2%	0.1%
0.15:0.15		0.15%	0.15%
0.1:0.2		0.1%	0.2%
0:0.3		0	0

2.2.2. Marshall Mix Design

Figure 2 shows the OGFC-13 gradation used in this research. According to the JTG F40-2004 standard, the OGFC-13 mix design was carried out using Marshall's design. The mix design results of OGFC-13 containing different fiber content and ratios are shown in Table 4.

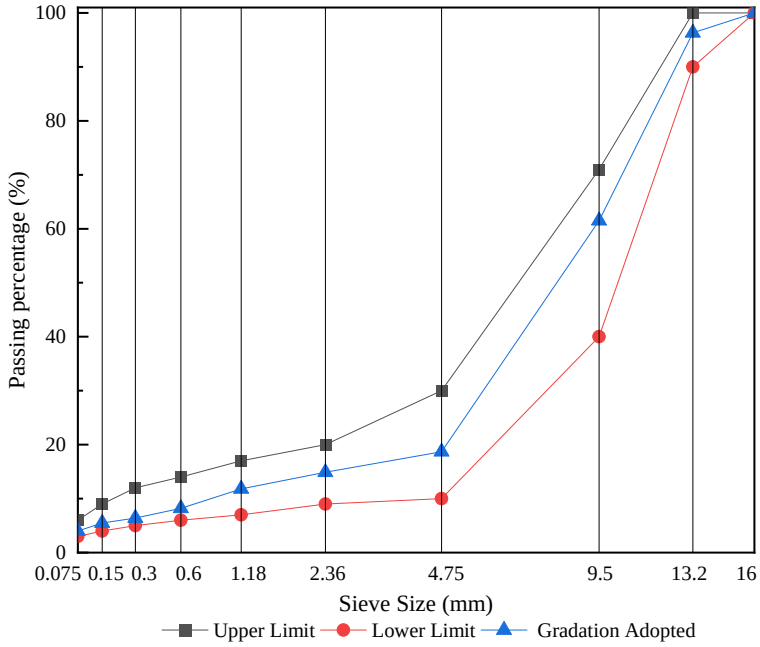

Figure 2. Mixes gradation.

Table 4. The mix design results of OGFC-13.

Group ID	Control	0.3:0	0.2:0.1	0.15:0.15	0.1:0.2	0:0.3
OAC (%)	4.50%	4.77%	4.71%	4.68%	4.61%	4.57%

2.3. Test Method

2.3.1. High-Temperature Performance Test

Based on the T0719 section in the Chinese Standard Test Methods of Bitumen and Bituminous Mixtures for Highway Engineering (JTG E20-2019) [26], the 300 mm × 300 mm × 50 mm rutting specimen used in this study was subjected to a wheel tracking test to determine its dynamic stability and evaluate the high-temperature rutting resistance performance of fibers in the OGFC-13 mixture. The test temperature was 60 °C, the loading pressure was 0.7 MPa, and the test time was 60 min. Equation (1) is used to calculate the dynamic stability (*DS*) value:

$$DS = \frac{(t_2 - t_1) \times N}{d_2 - d_1} \times C_1 \times C_2 \quad (1)$$

where t_1 and t_2 are the loading times of 45 min and 60 min. The parameters d_1 and d_2 represent the deformations at 45 min and 60 min. The parameter N is the round-trip rolling speed of the test wheel, set as 42 times/min. The parameter C_1 represents the coefficient of the testing machine type, and the reciprocating operation mode of the loading wheel driven by the crank connecting rod is 1.0. The parameter C_2 is the coefficient of the specimen size and is taken as 1.0 using a specimen with a width of 300 mm.

Moreover, the standard Marshall sample method was conducted to measure the 60 °C shearing strength R_τ with a universal testing machine (UTM). The loading head has a diameter of 28.5 mm and a height of 50 mm. The R_τ value is calculated by Equation (2). The detailed process is set out in the T0767 section of the JTG E20-2019 [26]:

$$R_\tau = f_\tau \frac{P}{A} \quad (2)$$

where f_τ is the shear stress coefficient, taken as 0.34 in this study; P and A are the ultimate load at specimen failure and the cross area of the loading head, respectively.

2.3.2. Low Temperature Bending Test

The low-temperature bending test was used to evaluate the low-temperature performance of OGFC-13 mixtures, as per the T0715 section in the JTG E20-2019 [26]. The 250 mm × 30 mm × 35 mm prism specimens used in this study were cut from a rutting specimen and loaded at a testing temperature of −10 °C and a loading rate of 50 mm/min by the UTM. The bending stress R_B and bending strain ε_B are determined by Equations (3) and (4):

$$R_B = \frac{3LP}{2bh^2} \tag{3}$$

$$\varepsilon_B = \frac{6hd}{L^2} \tag{4}$$

where L, b and h represent the specimen span, length and width of the middle section of the specimen, respectively; P and d correspond to the maximum load and mid-span deflection during specimen failure.

2.3.3. Water Stability Performance Test

The effect of the fiber ratio on the water stability performance was investigated using the Marshall immersion test and the freeze–thaw splitting test. The Marshall specimens were formed via double-sided compaction conducted 75 times in the Marshall immersion test, and Marshall stability (MS) was measured at 60 °C under a loading rate of 50 mm/min. In the freeze–thaw splitting test, the Marshall specimens were formed via double-sided compaction conducted 50 times and the splitting strength R_T at 25 °C was determined under a loading rate of 50 mm/min. The MS ratio and tensile strength ratios (TSR) were calculated based on Equations (5) and (6). More details about both of the methods are shown in sections T0709 of the Standard JTG E20-2019 [26] and AASHTO T 283 T245 [27], respectively.

$$MSR = \frac{MS_2}{MS_1} \times 100\% \tag{5}$$

$$TSR = \frac{R_{T2}}{R_{T1}} \times 100\% \tag{6}$$

where MS_2 and MS_1 correspond to the 30 min and 48 h MS values; R_{T1} and R_{T2} correspond to the splitting strength before and after the freeze–thaw cycle, respectively.

2.3.4. Cantabro Test

All standard Marshall samples were subjected to the Cantabro test, leading to an evaluation of the aggregate loss due to insufficient asphalt dosage or adhesion under traffic loads in accordance with ASTM C131 [28]. The Marshall specimens that were compacted 50 times were used in this study and tested at 20 °C. The stripping loss ΔS was determined by Equation (7):

$$\Delta S = \frac{m_0 - m_1}{m_0} \tag{7}$$

where m_0 and m_1 represent the mass of Marshall specimens before and after the test, respectively.

2.3.5. Indirect Tensile Fatigue Test

The indirect tensile fatigue test was performed on the cylindrical-shaped samples with a diameter of 101.6 ± 0.25 mm and a height of 63.5 ± 1.3 mm. A half-sine wave load was applied in the stress control mode of the UTM to replicate the recurring effect of loads on the road surface, with a load frequency of 10 Hz. The loading stress level S was defined as the ratio of the maximum cyclic stress to the ultimate indirect tensile strength and selected as 0.3, 0.4, 0.5 and 0.6, respectively. The test temperature was set at 15 °C ± 0.5 °C based on the Standard NEN-EN 12697-24 [29]. To better reflect reality, adjacent waveforms experienced intermittent periods, with a loading time of 0.01 s and an

intermittent time of 0.09 s within one cycle. Three parallel tests were carried out at each stress level.

2.3.6. Radar Chart Method

The radar chart method is used for comprehensive analysis when there are many factors to assess, and the evaluation results are clear and easy to calculate [30,31]. In this research, this method was adopted to determine the optimal composite fiber content by assessing the influence of the fiber ratio on the road performances, including high-temperature performance, low-temperature performance, fatigue performance, water stability and adhesion performance. In order to unify the units of different indicators, it is necessary to standardize each indicator. The standardized calculation formula is shown in Equation (8):

$$b_{ij} = \frac{a_{ij} - E(x_j)}{\sigma(y_j)} \tag{8}$$

$$E(x_j) = \frac{1}{k}\sum_{i=1}^{k} a_{ij} \tag{9}$$

$$\sigma(y_j) = \sqrt{\frac{\sum_{i=1}^{k}(a_{ij} - E(y_i))^2}{k}} \tag{10}$$

where i, j, a_{ij} and b_{ij} are the serial number of evaluated objects, the serial number of evaluation indices, the original index value and standardized values, respectively. $E(x_j)$ and $\sigma(y_j)$ are the mean and standard deviation of the jth indicator, calculated using Equations (9) and (10), respectively.

Next, all standardized values are converted into radians for displaying in the radar chart, as per Equation (11):

$$r_{ij} = \frac{2}{\pi}\arctan(b_{ij}) + 1 \tag{11}$$

where r_{ij} is the converted value. According to the calculated results, a radar chart can be drawn, as shown in Figure 3.

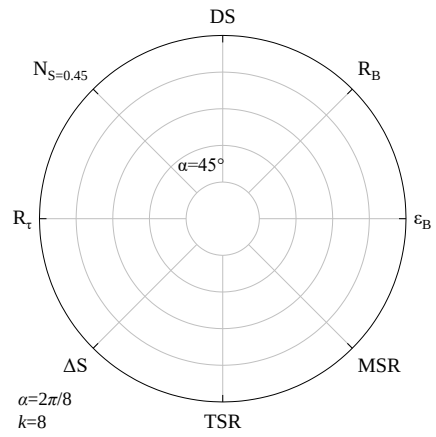

Figure 3. The radar chart.

Then, based on Equations (12) and (13), the area and perimeter of the radar chart are determined to evaluate the comprehensive performance of these asphalt mixes containing a different fiber ratio:

$$\begin{cases} A_i = \frac{\pi}{k}\sum_{j=1}^{k} r_{ij}^2 \\ L_i = \frac{2\pi}{k}\sum_{j=1}^{k} r_{ij} \end{cases} \tag{12}$$

$$f_i = \sqrt{\frac{A_i}{\max A_i} \times \frac{L_i}{2\sqrt{\pi A_i}}} \tag{13}$$

where *k* is the total number of evaluation indices.

3. Results and Discussion

3.1. High-Temperature Stability Evaluation

Figure 4 displays the 60 °C shearing strength and *DS* results of the different fiber-reinforced OGFC-13 mixes. The fibers noticeably enhance the high-temperature performance of the OGFC-13 mixtures due to their stabilizing and reinforcing effects on the asphalt and aggregates. As the GF content increased, the *DS* value also increased, while the shear strength showed a parabolic change. Compared to the control group, the *DS* values of OGFC-13 mixes corresponding to 0.3:0, 0.2:0.1, 0.15:0.15, 0.1:0.2 and 0:0.3 were enhanced by 17%, 20%, 33%, 44% and 51%, respectively. At the same time, the shearing strength accordingly improved by 14%, 21%, 30%, 27% and 25%. These results indicated that GF demonstrates a better improvement in high-temperature performance than LF due to its greater length and superior mechanical properties, which facilitate the formation of a reinforced network structure in the mixture [6,8,22]. The OGFC-13 mixes that were reinforced with two fibers have a lower *DS* value than those modified with single GF; meanwhile, single GF performed better than single LF. Moreover, the sample of LF:GF = 0.15:0.15 showed the best shearing strength, increasing by at least 3.5% more than that of the single fiber modification. In conclusion, the double-fiber modification method demonstrates outstanding resistance to rutting.

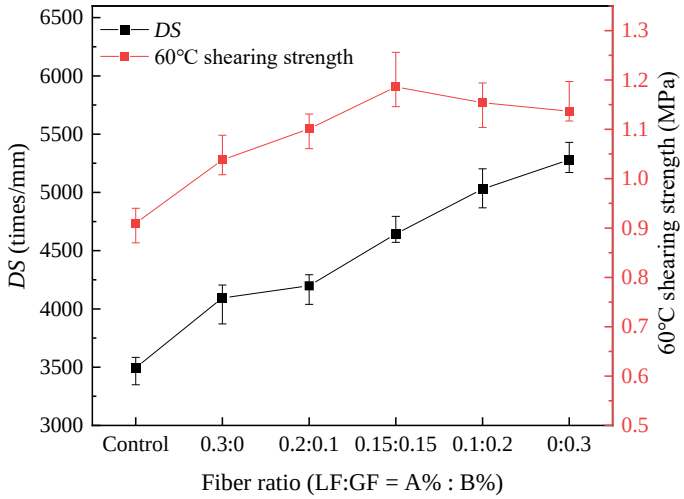

Figure 4. The test result of *DS* and shearing strength.

3.2. Low-Temperature Performance Evaluation

The test results of low-temperature performance evaluation are shown in Figure 5, which demonstrates the effectiveness of fibers in enhancing the low-temperature crack resistance of OGFC-13. Compared to the control samples, these OGFC-13 samples modified with different fiber ratios of 0.3:0, 0.2:0.1, 0.15:0.15, 0.1:0.2 and 0:0.3 enhanced with 12%, 18%, 27%, 26% and 28% in the bending strength, and having a 28%, 20%, 22%, 17% and 9% improvement in the bending strain, respectively. Similar to the high-temperature performance, the fibers also demonstrate a notable improvement in low-temperature performance. The fiber acts as steel reinforcement within the asphalt mixture [10,19]. Both fibers can improve the interfacial strength of the asphalt mixture and slow down fracture formation and expansion, therefore boosting the low-temperature crack resistance of OGFC-13.

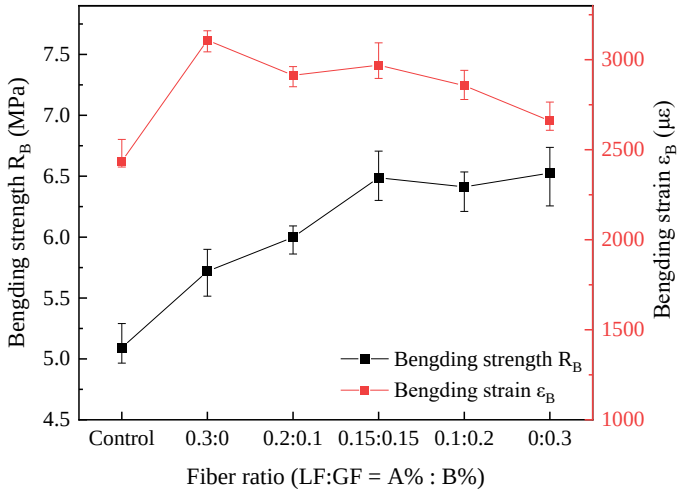

Figure 5. The test results of the low-temperature bending test.

Moreover, GF fiber-reinforced specimens exhibit better performance in bending stress. As shown in Table 2, the modulus and tensile strength of GF fiber are much higher than those of LF fiber, so GF-reinforced specimens performed better in bending stress. Compared with GF, LF has a larger specific surface area, stronger adsorption capacity for asphalt, and higher flexibility. It can effectively improve the deformation resistance of asphalt mixtures. Therefore, the OGFC-13 specimen modified with LF fiber has the highest flexural and tensile strain.

The OGFC-13 mix with a fiber ratio of 1.5:1.5 exhibits the best low-temperature performance among all OGFC-13 mixes using both fibers. Moreover, the OGFC-13 mix of LF:GF = 1.5:1.5 decreased by 4.5% in the bending strain and improved by 13% in bending stress in comparison with the single LF, while showing an equal low-temperature bending stress and increasing the 12% bending strain more than those of the single GF. It is clear that the two fibers work together to exert their respective advantages. LF uses its flexibility to create a flexible reinforcement network, while GF uses its strength to create a rigid reinforcement network, allowing the mixture to achieve optimal improvement in low-temperature performance.

3.3. Water Stability Evaluation

The test results of the Marshall immersion test and the freeze–thaw splitting test are shown in Figure 6. As can be seen, LF and GF enhance the strength of OGFC-13 mixtures, with GF showing superior performance in strength enhancement, aligning with the conclusion about shearing and bending strength. Those fiber-reinforced samples exhibited better MS_1, MS_2, R_{T1} and R_{T2} values than the samples without fibers, increasing by at least 13%, 26%, 9% and 15%, respectively. Moreover, both the *MSR* and *TSR* values show a similar parabolic trend as the fiber ratio change, reaching the maximum *MSR* value at LF:GF = 0.2:0.1 and the *TSR* value at LF:GF = 0.15:0.15, respectively. Compared with the samples without fibers, the *MSR* values increased by 11%, 12%, 10%, 6% and 7% as the fiber ratio changed from 0.3:0 to 0.3:0, and the *TSR* values improved by 5%, 9%, 11%, 9% and 8%, respectively. Obviously, LF and GF have a significant effect on improving the water stability of mixtures. The OGFC mixture's significant void structure can result in the asphalt coating on the aggregate surface being washed away by water erosion, causing a failure in aggregate adhesion. Adding fibers can absorb and stabilize the asphalt, improving the adhesive properties between particles. Fibers create a physical link between asphalt and aggregates, functioning as dowel bars to transmit and distribute stress in asphalt mixes [17,24]. The OGFC mixes using two additives of LF and GF exhibit better anti-water damage performance than those with a single fiber. This is also attributable to the different properties of the fibers [14]. Overall, the simultaneous addition of both LF

and GF demonstrated greater enhancement in moisture stability than the single-adding fiber technology.

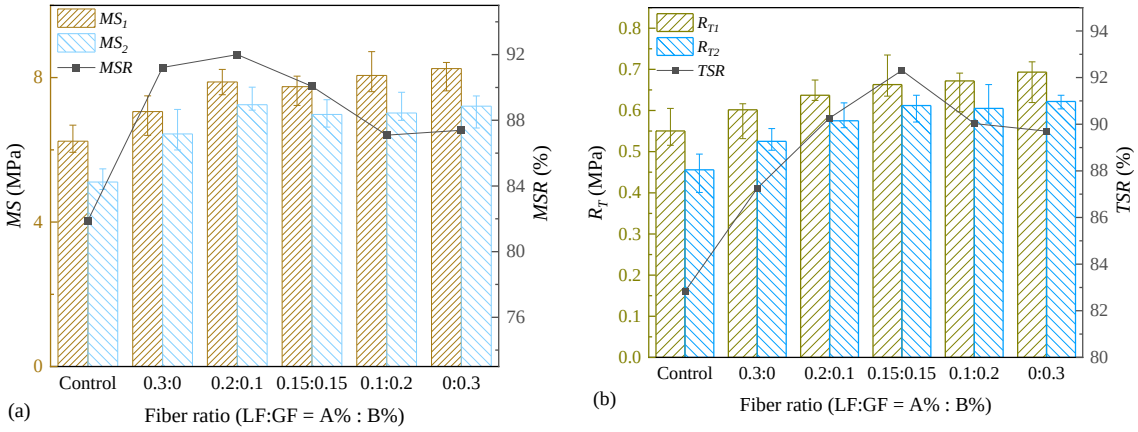

Figure 6. The results of water stability evaluation: (**a**) immersion Marshall test and (**b**) freeze–thaw splitting test.

3.4. Anti-Stripping Performance Evaluation

Approximately 75% of deterioration in OGFC pavements is attributed to stripping losses. The effectiveness of the permeable asphalt mixture directly impacts the drainage permeability and durability of permeable pavement [32]. Figure 7 depicts the influence of the ratio of LF to GF on the anti-stripping properties of the OGFC-13 mix. The stripping loss rose with the increase in the GF content, and the OGFC mix containing an LF and GF ratio of 3:0 showed the best anti-stripping performance. This is related to the fiber oil absorption capability. LF has numerous microscopic pores that facilitate the adsorption of asphalt, resulting in the highest adsorption capacity for asphalt. In contrast, GF has a smooth surface, which causes it to have a low adsorption capacity. The OGFC mix enhanced with the fibers reduced the stripping loss by a minimum of 9% compared to the control sample.

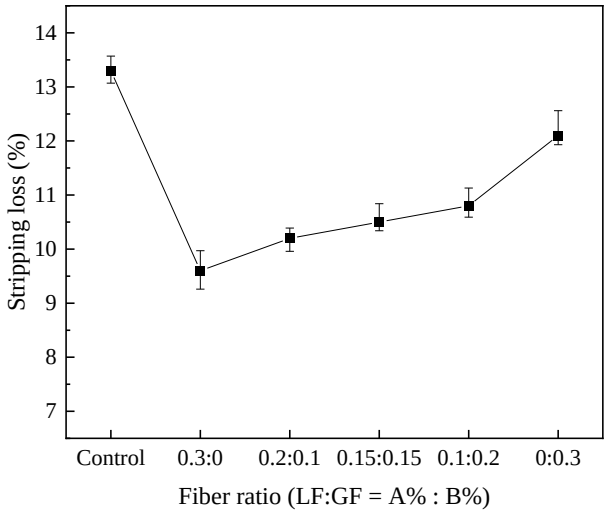

Figure 7. The test result of the Cantabro test.

3.5. Fatigue Performance Evaluation

The results of the 15 °C indirect tensile strength test and fatigue test of different fiber OGFC-13 samples are shown in Tables 5 and 6, respectively. Based on determining the loading stress level, the applied load value of the indirect tensile fatigue test depends on the indirect tensile fatigue strength of the specimen. Therefore, the indirect tensile strength tests are first conducted using the UTM.

Table 5. The results of 15 °C indirect tensile strength.

Fiber Ratio	Control	0.3:0	0.2:0.1	0.15:0.15	0.1:0.2	0:0.3
Splitting strength (MPa)	0.78	0.83	0.87	0.93	0.89	0.90

Table 6. Fatigue test results.

Fiber Ratio	*S*	The Fatigue Lives (*N*) Corresponding to Stress Ratio (*S*)			
		①	②	③	Mean
Control	0.3	8245	8922	9501	8889
	0.4	3311	3423	3197	3310
	0.5	1555	1347	1517	1473
	0.6	638	546	605	596
0.3:0	0.3	10,358	10,213	9462	10,011
	0.4	4496	5717	4814	5009
	0.5	1934	2072	2268	2091
	0.6	781	808	843	811
0.2:0.1	0.3	12,727	13,175	12,342	12,748
	0.4	5756	6094	6693	6181
	0.5	2875	2969	2026	2623
	0.6	1002	982	1157	1047
0.15:0.15	0.3	13,668	14,764	14,851	14,428
	0.4	6288	5931	6091	6103
	0.5	3098	3062	2865	3008
	0.6	1189	1203	1210	1201
0.1:0.2	0.3	17,888	15,487	13,566	15,647
	0.4	8024	6867	7557	7483
	0.5	2746	3122	3235	3034
	0.6	1292	1128	1410	1277
0:0.3	0.3	17,391	16,917	15,427	16,578
	0.4	8142	8534	8077	8251
	0.5	3574	3107	3322	3334
	0.6	1210	1259	1344	1271

Based on Tables 5 and 6, the experimental results show that the samples at LF:GF = 0.15:0.15 possess the best indirect tensile strength, increasing by 12% more than that of the single LF and by 3% more than that of the single GF, respectively. The fatigue life of different OGFC-13 samples decreased with the increasing loading stress, and there was a significant dispersion in fatigue life across different stress levels.

As shown in Equation (14), the double logarithmic equation was selected to characterize the form of the stress fatigue equation as follows [33,34]:

$$\lg N = -b\lg S + a \tag{14}$$

where N and S represent the fatigue life and stress level; a and b are the regression parameters. Among them, the value of a represents the intercept of the fatigue curve, indicating the fatigue resistance performance of the mixture, while the value of b represents the slope of the fatigue curve, indicating the sensitivity of the fatigue life of the specimen to stress changes. The larger the value of a and the smaller the value of b, the better the fatigue resistance of the mixture [33,35].

The influence of the fiber ratio on the fatigue equation parameters and fatigue curves are displayed in Figure 8 and Table 7, respectively. As shown in Figure 8 and Table 7, the fatigue life of the fiber-reinforced asphalt mixture decreased as the stress level increased, with a correlation coefficient over 0.97, demonstrating a strong relationship between fatigue life and strain level. Compared to the control group, the addition of LF and GF significantly

improves the fatigue performance of the OGFC-13 mix. The parameter *a* increased gradually as the ratio of LF:GF changed from 0.3:0 to 0:0.3, suggesting that GF exhibits superior fatigue life performance compared to LF. GF possesses superior strength, stiffness, and modulus, enhancing its ability to enhance the overall strength of mixtures and thereby extending the ultimate fatigue life under various stressors. Correspondingly, the parameter *b* showed a V-shaped trend with the decrease in GF content, reaching its minimum value at 0.15:0.15. This indicates that LF performs better than GF in relation to sensitivity to stress changes. Obviously, LF has a certain improvement effect on the crack resistance of the mixture and is more conducive to improving the toughness of the mixture, helping to slow down the expansion of cracks and reducing the impact of stress changes. Moreover, the double-adding fiber technology exhibits a lower sensitivity to stress changes compared to single-adding fiber technology.

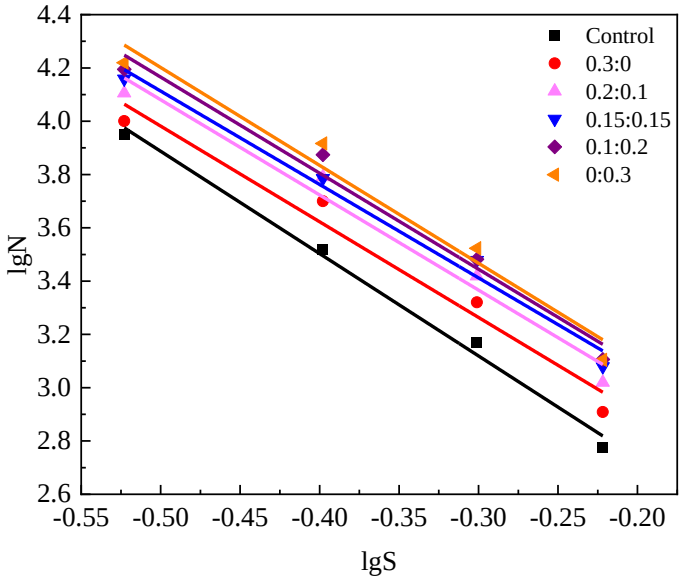

Figure 8. The fatigue curve.

Table 7. Fatigue equation parameters.

Fiber Ratio	*a*	*b*	R^2
Control	1.967	3.841	0.993
0.3:0	2.187	3.590	0.971
0.2:0.1	2.295	3.571	0.976
0.15:0.15	2.360	3.505	0.985
0.1:0.2	2.363	3.605	0.981
0:0.3	2.365	3.674	0.970

Previous studies have shown that a stress ratio of S = 0.45 is the critical point at which fatigue life N undergoes significant changes [33,35]. Table 8 lists the fatigue life at S = 0.45. As can be seen in Table 8, GF can effectively improve the fatigue life of OGFC-13, significantly increasing it by 61% compared to LF. As the GF content decreases, the fatigue life also gradually decreases. The OGFC-13 sample with a fiber ratio of 0.1:0.2 has the second-highest fatigue life among all samples. When the glass fiber content is low, the strength of the fiber network skeleton drops, leading to a less noticeable reinforcement effect.

Table 8. The results of fatigue life at S = 0.45.

Fiber Ratio	Control	0.3:0	0.2:0.1	0.15:0.15	0.1:0.2	0:0.3
Fatigue life (times)	1990	2702	3415	3768	4104	4354

3.6. Comprehensive Performance Evaluation

The above experimental results indicate that different fiber ratios have varying effects on the various road performances of the mixture. This study used the radar chart method to comprehensively evaluate the impact of different fiber ratios on the overall road performances of OGFC-13. A total of eight indicators were selected, including dynamic stability *DS*, bending strength R_B, bending strain ε_B, *MSR*, *TSR*, stripping loss ΔS, shearing strength R_τ and fatigue life at $S = 0.45$. It should be noted that the stripping loss must be transformed into the percentage of scattered residual mass when calculating the process. This percentage represents the largest piece in the residual specimen after the test compared to the entire mass of the original specimen. Table 9 presents the r_{ij} values calculated from Equations (8)–(11). Furthermore, the radar charts of different OGFC-13 mixes were drawn, as shown in Figure 9. As can be seen, the control mixes show the worst overall performance and the OGFC-13 modified by the double-adding technology performed better and showed more balance in the overall road performance than those samples containing a single fiber.

Table 9. The r_{ij} results.

Fiber Ratio	The Standardized Value r_{ij} of Different Evaluation Indicators							
	DS	**R_B**	**ε_B**	**MSR**	**TSR**	**ΔS**	**Rτ**	**$N_{S=0.45}$**
Control	0.315	0.319	0.342	0.310	0.301	0.326	0.317	0.337
0.3:0	0.767	0.641	1.624	1.455	0.710	1.555	0.568	0.555
0.2:0.1	0.863	0.937	1.041	1.531	1.299	1.392	1.188	1.020
0.15:0.15	1.221	1.442	1.372	1.309	1.553	1.278	1.480	1.276
0.1:0.2	1.458	1.384	1.104	0.786	1.258	1.142	1.422	1.457
0:0.3	1.561	1.512	0.612	0.837	1.198	0.565	1.354	1.552

Based on Table 9, the final comprehensive scores were summarized as per Equations (12) and (13). The comprehensive scores of the six OGFC-13 mixes are rated in the following order: control group < 0.3:0 < 0.2:0.1 < 0:0.3 < 0.1:0.2 < 0.15:0.15, as shown in Table 10. These results clearly show that the double-adding technology shows the best improvement in overall road performance, and the performance rankings of the three asphalt mixtures modified by two fibers are also provided. OGFC-13 mixtures with different LF and GF contents have their own advantages and disadvantages in various aspects of road performance. The findings provide important guidance for choosing fiber ratios according to specific performance goals in various application situations, highlighting the need to use dual-fiber modifications to enhance asphalt mix performance.

Table 10. The comprehensive scores of the radar chart method.

Fiber Ratio	Control	0.3:0	0.2:0.1	0.15:0.15	0.1:0.2	0:0.3
L value	2.016	6.185	7.282	8.586	7.863	7.220
A value	0.324	3.654	4.370	5.904	5.070	4.633
f value	0.234	0.752	0.853	0.998	0.920	0.862

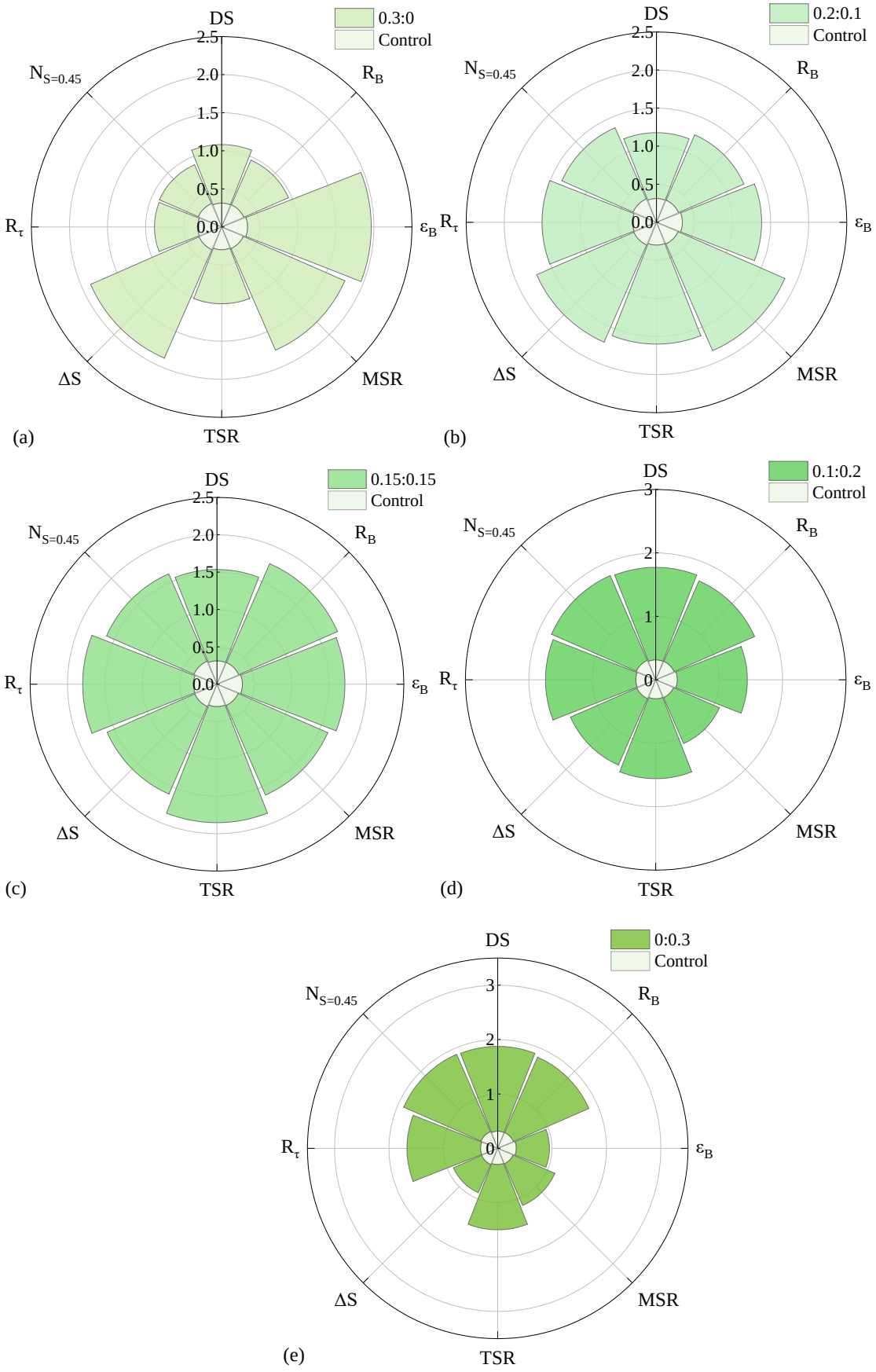

Figure 9. The radar chart of six OGFC-13 mixes: (**a**) 0.3:0; (**b**) 0.2:0.1; (**c**) 0.15:0.15; (**d**) 0.1:0.2; (**e**) 0:0.3.

4. Conclusions

This study examines the effect of double-adding technology for lignin and glass fibers on the road performances shown by OGFC mixes. Based on extensive laboratory experiments, the brief conclusions are set out below:

(1) The addition of GF and LF significantly improves the high-temperature performance of OGFC-13 mixes. The DS values increased with the GF content while shearing strength reached a peak in the LF:GF = 0.15:0.15 ratio. The double-fiber modification technology demonstrated a more balanced high-temperature performance than single-fiber modifications.

(2) Both fibers effectively enhanced the low-temperature crack resistance of OGFC-13 mixes. GF-reinforced specimens performed better in bending stress, while LF-reinforced specimens had the highest flexural strain.

(3) Both LF and GF significantly improved the water stability of OGFC-13 mixes. LF and GF had a substantial effect on enhancing MS_1, MS_2, RT_1 and RT_2 values in Marshall immersion and freeze–thaw splitting tests. The simultaneous addition of both LF and GF demonstrated a better improvement in moisture stability compared to single-fiber technology.

(4) The anti-stripping performance of OGFC-13 mixes modified with fibers was significantly better than the control group. The LF:GF = 3:0 ratio showed the best anti-stripping performance, attributed to LF's strong asphalt adsorption capacity.

(5) Both LF and GF enhanced the fatigue performance of OGFC-13 mixes, with GF performing better in fatigue life than LF. The LF:GF = 0.15:0.15 ratio exhibited a balanced fatigue performance. The double-adding fiber technology showed a lower sensitivity to stress changes compared to the single-adding fiber technology.

(6) A comprehensive road performance evaluation using the radar chart method showed that the double-adding technology exhibits a well-rounded enhancement in overall road performance. The ratio of LF:GF = 0.15:0.15 was determined to have the most optimal road performance out of all the ratios examined. This study proposes that the optimal fiber ratio can be chosen according to specific performance objectives in various application scenarios.

Author Contributions: Conceptualization, H.Z.; methodology, W.L. and H.L.; investigation, S.Z. and W.L.; resources, C.C., C.L. and S.Z.; data curation, S.Z. and W.L.; writing—original draft preparation, W.L. and H.L.; writing—review and editing, H.L.; supervision, H.L. and H.Z.; project administration, C.C., C.L. and H.Z.; funding acquisition, C.C., C.L. and H.Z. All authors have read and agreed to the published version of the manuscript.

Funding: This work was supported by the Science and Technology Innovation Demonstration Project of the Transportation Department of Yunnan Province (Science and Technology Education Section of Transport Department of Yunnan Province [2019] No. 14).

Data Availability Statement: The data presented in this study are available on request from the corresponding author. The data are not publicly available due to commercial privacy.

Conflicts of Interest: Cihe Chen, Chimou Li were employed by Wenshan Expressway Construction and Development of CCCC Co., Ltd.; Cihe Chen was employed by CCCC Western Investment Co., Ltd.; Chimou Li was employed by CCCC Second Harbor Engineering Company Ltd.; Saibang Zhang was employed by Yunnan Wenshan Transportation Investment Group Engineering Quality Testing Co., Ltd.; Wenchang Liu was employed by Shanghai Fengxian Construction Development Group Co., Ltd. The remaining authors declare that the research was conducted in the absence of any commercial or financial relationships that could be construed as a potential conflict of interest.

References

1. Hu, M.; Li, L.; Peng, F. Laboratory investigation of OGFC-5 porous asphalt ultra-thin wearing course. *Constr. Build. Mater.* **2019**, *219*, 101–110. [CrossRef]
2. Alvarez, A.E.; Martin, A.E.; Estakhri, C. Internal structure of compacted permeable friction course mixtures. *Constr. Build. Mater.* **2010**, *24*, 1027–1035. [CrossRef]

3. Zhang, J.W.; Huang, W.D.; Zhang, Y.; Lv, Q.; Yan, C.Q. Evaluating four typical fibers used for OGFC mixture modification regarding drainage, raveling, rutting and fatigue resistance. *Constr. Build. Mater.* **2020**, *253*, 119131. [CrossRef]
4. Shahnewaz, S.M.; Masri, K.A.; Ahmad Abdul Ghani, N.A.; Putra Jaya, R.; Siew Choo, C.; Giannakopoulou, P.P.; Rogkala, A.; Lampropoulou, P.; Petrounias, P. Porous asphalt mixtures enriched with bamboo fibers as a new approach for future sustainable construction. *Constr. Build. Mater.* **2023**, *407*, 133456. [CrossRef]
5. Phan, T.M.; Nguyen, S.N.; Seo, C.-B.; Park, D.-W. Effect of treated fibers on performance of asphalt mixture. *Constr. Build. Mater.* **2021**, *274*, 122051. [CrossRef]
6. Abtahi, S.M.; Sheikhzadeh, M.; Hejazi, S.M. Fiber-reinforced asphalt-concrete—A review. *Constr. Build. Mater.* **2010**, *24*, 871–877. [CrossRef]
7. Kou, C.; Chen, Z.; Kang, A.; Zhang, M.; Wang, R. Rheological behaviors of asphalt binders reinforced by various fibers. *Constr. Build. Mater.* **2022**, *323*, 126626. [CrossRef]
8. Xing, X.; Chen, S.; Li, Y.; Pei, J.; Zhang, J.; Wen, Y.; Li, R.; Cui, S. Effect of different fibers on the properties of asphalt mastics. *Constr. Build. Mater.* **2020**, *262*, 120005. [CrossRef]
9. Partl, M.N.; Vinson, T.S.; Hicks, R.G. Mechanical properties of stone mastic asphalt. In *Infrastructure: New Materials and Methods of Repair*; ASCE: Reston, VA, USA, 1994; pp. 849–858.
10. Abdelaziz, M.; Katman, H. Prospect of using glass fiber reinforced bituminous mixes. *J. East. Asia Soc. Transp. Stud.* **2003**, *5*, 794–807.
11. Lastra-González, P.; Calzada-Pérez, M.A.; Castro-Fresno, D.; Vega-Zamanillo, Á.; Indacoechea-Vega, I. Comparative analysis of the performance of asphalt concretes modified by dry way with polymeric waste. *Constr. Build. Mater.* **2016**, *112*, 1133–1140. [CrossRef]
12. Rodríguez-Fernández, I.; Tarpoudi Baheri, F.; Cavalli, M.C.; Poulikakos, L.D.; Bueno, M. Microstructure analysis and mechanical performance of crumb rubber modified asphalt concrete using the dry process. *Constr. Build. Mater.* **2020**, *259*, 119662. [CrossRef]
13. Fu, Z.; Shen, W.; Huang, Y.; Hang, G.; Li, X. Laboratory evaluation of pavement performance using modified asphalt mixture with a new composite reinforcing material. *Int. J. Pavement Res. Technol.* **2017**, *10*, 507–516. [CrossRef]
14. Li, J.; Yang, L.; He, L.; Guo, R.; Li, X.; Chen, Y.; Muhammad, Y.; Liu, Y. Research progresses of fibers in asphalt and cement materials: A review. *J. Road Eng.* **2023**, *3*, 35–70. [CrossRef]
15. Guo, F.; Li, R.; Lu, S.; Bi, Y.; He, H. Evaluation of the Effect of Fiber Type, Length, and Content on Asphalt Properties and Asphalt Mixture Performance. *Materials* **2020**, *13*, 1556. [CrossRef] [PubMed]
16. Kou, C.; Wu, X.; Xiao, P.; Liu, Y.; Wu, Z. Physical, Rheological, and Morphological Properties of Asphalt Reinforced by Basalt Fiber and Lignin Fiber. *Materials* **2020**, *13*, 2520. [CrossRef] [PubMed]
17. Khater, A.; Luo, D.; Abdelsalam, M.; Yue, Y.; Hou, Y.; Ghazy, M. Laboratory Evaluation of Asphalt Mixture Performance Using Composite Admixtures of Lignin and Glass Fibers. *Appl. Sci.* **2021**, *11*, 364. [CrossRef]
18. Sun, T. *Research on the Influence of Fiber Blending on the Road Performance of SMA Asphalt Mixture*; Chongqing Jiaotong University: Chongqing, China, 2020.
19. Abtahi, S.M.; Esfandiarpour, S.; Kunt, M.; Hejazi, S.M.; Ebrahimi, M.G. Hybrid reinforcement of asphalt-concrete mixtures using glass and polypropylene fibers. *J. Eng. Fibers Fabr.* **2013**, *8*, 155892501300800203. [CrossRef]
20. Chegenizadeh, A.; Peters, B.; Nikraz, H. Mechanical properties of stone mastic asphalt containing high-density polyethene: An Australian case. *Case Stud. Constr. Mater.* **2021**, *15*, e00631. [CrossRef]
21. Enieb, M.; Diab, A.; Yang, X. Short- and long-term properties of glass fiber reinforced asphalt mixtures. *Int. J. Pavement Eng.* **2021**, *22*, 64–76. [CrossRef]
22. Zhao, H.; Guan, B.; Xiong, R.; Zhang, A. Investigation of the Performance of Basalt Fiber Reinforced Asphalt Mixture. *Appl. Sci.* **2020**, *10*, 1561. [CrossRef]
23. Mashaan, N.; Karim, M.; Khodary, F.; Saboo, N.; Milad, A. Bituminous Pavement Reinforcement with Fiber: A Review. *CivilEng* **2021**, *2*, 599–611. [CrossRef]
24. Miao, Y.; Wang, T.; Wang, L. Influences of Interface Properties on the Performance of Fiber-Reinforced Asphalt Binder. *Polymers* **2019**, *11*, 542. [CrossRef]
25. *JTG F40-2004*; Technical Standards of the Chinese Technical Specifications for Construction of Highway Asphalt Pavements. National Standards of the People's Republic of China: Beijing, China, 2004.
26. *JTG E20-2019*; Standard Test Methods of Bitumen and Bituminous Mixtures for Highway Engineering. National Standards of the People's Republic of China: Beijing, China, 2019.
27. *AASHTO. T283*; Resistance of Compacted Hot Mix Asphalt (HMA) to Moisture-Induced Damage. The National Academies Press: Washington, DC, USA, 2010.
28. *ASTM C131*; Test Method for Resistance to Degradation of Small-Size Coarse Aggregate by Abrasion and Impact in the Los Angeles Machine. ASTM: West Conshohocken, PA, USA, 2013.
29. *NEN-EN 12697-24*; Bituminous mixtures. Test Methods—Part 24: Resistance to Fatigue, Technical Committee CEN/TC 227 "Road Materials". Linked Standards Committee for Road Construction Materials: Brussels, Belgium, 2018.
30. Zhang, H.; Hou, Y.; Zhang, J.; Qi, X.; Wang, F. A new method for nondestructive quality evaluation of the resistance spot welding based on the radar chart method and the decision tree classifier. *Int. J. Adv. Manuf. Technol.* **2015**, *78*, 841–851. [CrossRef]

31. Du, X.; Teng, G.; Du, X.; Liu, M.L.; Wang, C.Y. Comprehensive evaluation of environmental comfort in layer poultry house using radar graph. *Trans. Chin. Soc. Agric. Eng.* **2020**, *36*, 202–209.
32. Zhang, J.; Huang, W.; Zhang, Y.; Cai, Q.; Yan, C.; Lv, Q. Investigation on the durability of OGFC-5 ultra-thin friction course with different mixes. *Constr. Build. Mater.* **2021**, *288*, 123049. [CrossRef]
33. Jiang, Y.; Lin, H.; Han, Z.; Deng, C. Fatigue Properties of Cold-Recycled Emulsified Asphalt Mixtures Fabricated by Different Compaction Methods. *Sustainability* **2019**, *11*, 3483. [CrossRef]
34. Jiang, Y.; Zhang, Y.; Xue, J.; Deng, C.; Tian, T. Performance of Stone Mastic Asphalt Mixtures Fabricated by Different Compaction Methods. *Appl. Sci.* **2020**, *10*, 2523. [CrossRef]
35. Xu, Y.; Jiang, Y.; Xue, J.; Ren, J. Investigating the Effect of Aggregate Characteristics on the Macroscopic and Microscopic Fracture Mechanisms of Asphalt Concrete at Low-Temperature. *Materials* **2019**, *12*, 2675. [CrossRef] [PubMed]